

The LOFAR Beam Former: Implementation and Performance Analysis

Jan David Mol, John W. Romein and Rob V. van Nieuwpoort

Stichting ASTRON (Netherlands Institute for Radio Astronomy)
Oude Hoogeveensedijk 4, 7991 PD Dwingeloo, The Netherlands
{mol,romein,nieuwpoort}@astron.nl

Abstract. Radio telescopes typically use large steel dishes to point at and observe radio sources. The LOFAR radio telescope is different, and uses tens of thousands of fixed antennas instead, a novel design which allows many groundbreaking features for radio astronomy. One such a feature is the fact that LOFAR observes omnidirectionally, and focusses by accumulating the signals of its antennas in software in real time. In fact, the parallel processing power and high-speed interconnect in our supercomputer allows us to look at hundreds of sources at the same time.

LOFAR is also the first major telescope to process its data in software, instead of needing a dedicated hardware design. By using software, the processing remains flexible and scalable, and new features are easier to implement and to maintain. It is through the use of software that we can fully explore the novel features and the power of our unique instrument.

In this paper, we present our processing pipeline which enables parallel observations. The pipeline receives up to 198 Gb/s, and performs signal-processing techniques, weighted addition, and two all-to-all exchanges, and outputs up to 80 Gb/s. We present the trade-offs in our design, the CPU and I/O performance bottlenecks that we encounter, as well as the scaling characteristics and its real-time behaviour.

1 Introduction

The LOFAR (LOW Frequency ARray) telescope is the first of a new generation of radio telescopes. Instead of using a set of large, expensive dishes, LOFAR uses many thousands of simple antennas. Every antenna observes the full sky, and the telescope can be aimed through signal processing techniques. LOFAR's novel design allows the telescope to perform wide-angle observations as well as to observe in multiple directions simultaneously, neither of which are possible when using traditional dishes. In several ways, LOFAR will be the largest telescope in the world, and will enable groundbreaking research in several areas of astronomy and particle physics [1].

Another novelty is the elaborate use of software to process the telescope data in real time. Previous generations of telescopes depended on custom-made hardware to combine data, because of the high data rates and processing requirements. The availability of sufficiently powerful supercomputers however, allow the use of software to combine telescope data, creating a more flexible and reconfigurable instrument.

For processing LOFAR data, we use an IBM BlueGene/P (BG/P) supercomputer. The LOFAR antennas are grouped into stations, and each station sends its data (up to 198 Gb/s for all stations) to the BG/P super computer. Inside the BG/P, the data are split and recombined using both real-time signal processing routines as well as two all-to-all exchanges. The output data streams are sufficiently reduced in size in order to be able to stream them out of the BG/P and store them on disks in our storage cluster.

The stations can be configured to observe in several directions in parallel, but have to divide their output bandwidth among them. In this paper, we present the *beamformer*, an extension to the LOFAR software which allows the telescope to be aimed in tens of directions simultaneously at LOFAR's full observational bandwidth, and in hundreds of directions at reduced bandwidth. Both feats cannot be matched by any other telescope. The data streams corresponding to each observational direction, called *beams*, are generated through (weighted) summations of the station inputs, which are demultiplexed using an all-to-all exchange, and routed to the storage cluster.

The primary scientific use case driving the work presented in this paper is pulsar research. A pulsar is a rapidly rotating, highly magnetised neutron star, which emits electromagnetic radiation from its poles. Similar to the behaviour of a lighthouse, the radiation is visible to us only if one of the poles points towards Earth, and subsequently appears to us as a very regular series of pulses, with a period as low as 1.4 ms [2]. Pulsars are relatively weak radio sources, and their individual pulses often do not rise above the background noise that fills our universe. LOFAR is one of the few telescopes which operates in the frequency range (10 – 240 MHz) in which pulsars are typically at their brightest. Our beamformer also makes LOFAR the only telescope that can observe in hundreds of directions simultaneously with high sensitivity. These aspects make LOFAR an ideal instrument to discover unknown pulsars by doing a sensitive sky survey in a short amount of time, as well as an ideal instrument to study known pulsars in more detail. Astronomers can also use our beamformer to focus on planets, exoplanets, the sun, and other radio objects, with unprecedented sensitivity. Furthermore, our pipeline allows fast broad-sky surveys to discover not only new pulsars but also other radio sources.

In this paper, we will show how a software solution and the use of massive parallelism allows us to achieve this feat. We provide an in-depth study on all performance aspects, real-time behaviour, and scaling characteristics. The paper is organised as follows.

2 Related Work

MWA.

LOFAR imaging pipeline [5]

3 LOFAR

The LOFAR telescope consists of many thousands of simple dipole antennas (see Figure 1(a)), grouped in *stations*. The stations are strategically placed, with 20 stations acting as its center (the *core*) and 24 stations at increasing distances from that core (see Figure

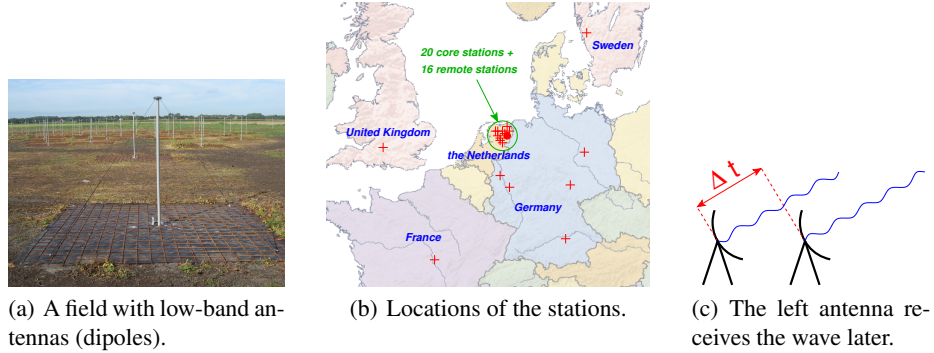


Fig. 1. LOFAR antennas

1(b)). A core station can act as two individual stations in some observational modes. Every station collects and combines the signals from its antennas, and sends the resulting data stream to our IBM BlueGene/P (BG/P) supercomputer at our central processing facility. The BG/P combines the data streams from one or more stations and reduces the resulting stream in size sufficiently to be able to store it on disks in our storage cluster. Both the stations and the BG/P perform hard-real-time signal processing. Once the data has been stored on disk, off-line processing takes over. The off-line processing transforms and further reduces the data produced by the BG/P into data products such as images or time series, and are made available to the astronomer(s) that requested the observation.

The antennas are omnidirectional and have no moving parts. Instead, all telescope functions are performed electronically through signal processing done at the stations and on the BG/P. The telescope can be aimed because the speed of light is finite: the light emitted by a source will arrive at different antennas at different times (see Figure 1(c)). By adding appropriate delays to the signals from individual antennas before accumulating them, the signals from the source will be amplified with respect to signals from other directions. Once the samples from all antennas are combined, the data are transmitted to the BG/P, which uses the same technique to combine the data from the individual stations. The latter will be explained further in Section 5.

A LOFAR station is able to produce 248 frequency subbands of 195 kHz out of the sensitivity range of 80 MHz to 250 MHz. Each sample consists of two complex 16-bit integers, representing the amplitude and phase of the X and Y polarizations of the antennas. The resulting data stream from a station is a 3.1 Gb/s UDP stream.

4 IBM BlueGene/P

We use an IBM BlueGene/P (BG/P) supercomputer for the real-time processing of station data. We will describe the key features of the BG/P, but more information can be found elsewhere [6]. Furthermore, we will describe how our BG/P is connected to its input and output systems.

4.1 System Description

Our system consists of 3 racks, with 12,480 processor cores that provide 42.4 TFLOPS peak processing power. One chip contains four PowerPC 450 cores, running at a modest 850 Mhz clock speed to reduce power consumption and to increase package density. Each core has two floating-point units (FPUs) that provide support for operations on complex numbers. The chips are organised in *psets*, each of which consists of 64 cores for computation (*compute cores*) and one chip for communication (*I/O node*). Each compute core runs a fast, simple, single-process kernel, and has access to 512 MiB of memory. The I/O nodes consist of the same hardware as the compute nodes, but additionally have a 10 Gb/s Ethernet interface connected. They run Linux, which allows the I/O nodes to do full multitasking. One rack contains 64 *psets*, which is equal to 4096 compute cores and 64 I/O nodes.

The BG/P contains several networks. A fast *3-dimensional torus* connects all compute nodes and is used for point-to-point and all-to-all communications over 3.4 Gb/s links. The torus uses DMA to offload the CPUs and allows asynchronous communication. The *collective network* is used for communication within a *pset* between an I/O node and the compute nodes, using 6.8 Gb/s links. In both networks, data is routed through compute nodes using a shortest path. Additional networks exist for fast barriers, initialization, diagnostics, and debugging.

4.2 External I/O

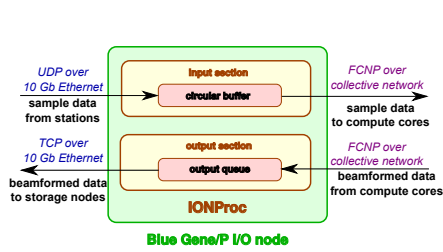


Fig. 2. Data flow diagram for the I/O nodes.

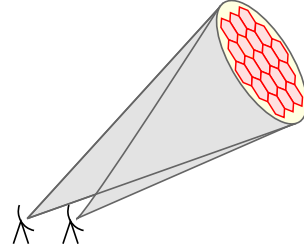


Fig. 3. Tied-array beams (hexagons) formed within a station beam (ellipse).

We customised the I/O node software stack [7] and run a multi-threaded program on each I/O node which is responsible for two tasks: the handling of input, and the handling of output (see Figure 2). Even though the I/O nodes each have a 10 Gb/s Ethernet interface, they do not have enough computation power to handle 10 Gb/s of data. The overhead of handling IRQs, IP, and UDP/TCP put a high load on the 850 MHz cores of the I/O nodes, limiting performance. An I/O node can output at most 3.1 Gb/s, unless it has to handle station input (3.1 Gb/s), in which case it can output at most 1.1 Gb/s. We implemented a low-overhead communication protocol called FCNP [4] to efficiently transport data to and from the compute nodes. Each I/O node forwards

its data to the compute nodes, which perform all of the necessary processing. Once the compute nodes have finished processing the data, the results are sent back to the I/O nodes. The I/O nodes forward these results to our storage cluster, which can sustain a throughput up to 80 Gb/s. The I/O node drops output data if it cannot be sent, in order to keep the system running at real time.

5 Beam Forming

A station focusses at a source by applying different delays to the signals from its antennas, and subsequently adding the delayed signals. Delaying the signals is known as *delay compensation*, and subsequently adding them as *beam forming*. The station beam former is implemented in hardware, in which the signal is delayed by switching it over wires of different lengths. The signals from the different antennas are subsequently added using an FPGA. The resulting *station beam*, even though it is focussed on a certain source, still has a wide field of view.

The BG/P, which receives the signals from all stations, again performs delay compensation and beam forming, this time in software. The BG/P beam former can focus on sources anywhere in the fields of view of the station beams, creating *tied-array beams* (beams). An example is shown in Figure 3, in which a station beam (represented by an ellipse) contains several tied-array beams (represented by hexagons). The actual width of the station beam, as well as the width of the tied-array beams, depends on the number as well as the locations of the stations used. Hundreds of tied-array beams are typically needed to fully cover the field of view of a station beam.

Different tied-array beams are created by adding the signals from the individual stations using different delays. The delays that have to be applied to obtain a tied-array beam depends on the relative positions of the stations and the relative direction of the tied-array beam with respect to the station beam. The delays are applied in two phases. First, the streams are aligned by shifting them a whole number of samples with respect to each other, which resolves delay differences up to the granularity of a single sample. Then, the remaining sub-sample delays are compensated for by shifting the phase of the signal. In order to obtain different tied-array beams, only the sub-sample delays have to be adjusted. A phase shift is performed by applying a complex multiplication. To form a beam, the beam former gathers the streams of samples from the stations, multiplies them with precomputed weights representing the required phase shift, and adds the streams together. The same weights are applied to both the X and the Y polarisations. The resulting data stream is called the *XY polarisations*, and consists of 32-bit complex floating point numbers (complex floats).

The XY polarisations can optionally be converted into *Stokes IQUV* parameters, which represent the polarisation aspects in an alternative way. The Stokes parameters are defined as $I = X\bar{X} + Y\bar{Y}$, $Q = X\bar{X} - Y\bar{Y}$, $U = 2\text{Re}(X\bar{Y})$, $V = 2\text{Im}(X\bar{Y})$, with each parameter being a 32-bit floats.

Both the XY polarisations and the Stokes IQUV parameters require up to 6.2 Gb/s per beam, which severely limits the number of beams that can be produced, and which represents a time resolution which is not always necessary. For example, in sky surveys, it is desirable to create many beams. The data rate per beam thus has to be lowered.

For many-beam observations, we convert the XY polarisations into just the *Stokes I* parameter, which represents the amplitude of the signal in the X and Y polarisations combined. The resulting data rate is 1.5 Gb/s per beam, but we also allow time-wise integration to further reduce the data rate with an integer factor, allowing even more beams to be created.

For each beam, each polarisation or Stokes parameter is stored in a separate file. If too many I/O nodes are limited to 1.1 Gb/s of output, full polarisation or Stokes parameter streams are too wide to transport. In such cases, we split the streams into *slices* of 83 or 124 subbands per substream instead of 248.

6 Pulsar Pipeline

In this section, we will describe in detail how the full signal-processing pipeline operates, in and around the beamformer. The use of a software pipeline allows us to reconfigure the components and design of our standard imaging pipeline, described in [5]. In fact, both pipelines can be run simultaneously.

6.1 Input from Stations

The first step in the pipeline is receiving and collecting from the stations on the I/O nodes. Each I/O node receives the data of (at most) one station, and stores the received data in a circular buffer (recall Figure 2). If necessary, the read pointer of the circular buffer is shifted a number of samples to reflect the coarse-grain delay compensation that will be necessary to align the streams from different stations.

The station data are split into chunks of one subband and approximately 0.25 seconds. The chunk size is chosen such that the compute cores have enough memory to perform all of the necessary processing. Due to the BG/P design, an I/O node sends chunks to its own compute cores only. The compute cores exchange the chunks they obtain from their I/O node using an all-to-all exchange.

6.2 First All-to-all Exchange

The first all-to-all exchange in the pipeline allows the compute cores to distribute the chunks from a single station, and to collect all the chunks of the same subband from all of the stations. The exchange is performed over the fast 3D-torus network, but with up to 198 Gb/s of station data to be exchanged (64 stations producing 3.1 Gb/s), special care still has to be taken to avoid network bottlenecks. It is impossible to optimise for short network paths due to the physical distances between the different psets across a BG/P rack. Instead, we optimised the data exchange by creating as many paths as possible between compute cores that have to exchange data. Within each pset, we employ a virtual remapping such that the number of possible routes between communicating cores in different psets is maximised.

The communications in the all-to-all exchange are asynchronous, which allows a compute core to start processing a subband from a station as soon as it arrives, up to the point that data from all stations are required. Communication and computation are thus overlapped as much as possible.

6.3 Signal Processing

Once a compute core receives a chunk, it can start processing. First, we convert the station data from 16-bit little-endian integers to 32-bit big-endian floats, in order to be able to do further processing using the powerful dual FPU units present in each core. The data doubles in size, which is the main reason why we implement it *after* the exchange.

Next, the data are filtered by applying a Poly-Phase Filter (PPF) bank, which consists of a Finite Impulse Response (FIR) filter and a Fast-Fourier Transform (FFT). The FFT allows the chunk, which represents a subband of 195 kHz, to be split into narrower subbands (*channels*). A higher frequency resolution allows more precise corrections in the frequency domain, such as the removal of radio interference at very specific frequencies.

Next, fine-grain delay compensation is performed to align the chunks from the different stations to the same source at which the stations are pointed. The fine-grain delay compensation is performed as a phase rotation, which is implemented as one complex multiplication per sample. The exact delays are computed for the begin time and end time of a chunk, and interpolated in frequency and time for each individual sample.

Next, a band pass correction is applied to adjust the signal strengths in all channels. This is necessary, because the stations introduce a bias in the signal strengths across the channels within a subband.

Up to this point, processing chunks from different stations can be done independently, but from here on, the data from all stations are required. The first all-to-all exchange thus ends here.

6.4 Beam Forming

The beamformer creates the beams as described in Section 5. First, the different weights required for the different beams are computed, based on the station positions and the beam directions. Note that the data in the chunks are already delay compensated with respect to the source at which the stations are pointed. Any delay compensation performed by the beamformer is therefore to compensate the delay differences between the desired beams and the station's source. The reason for this two-stage approach is flexibility. By already compensating for the station's source in the previous step, the resulting data can not only be fed to the beamformer, but also to other pipelines, such as the imaging pipeline. Because we have a software pipeline, we can implement and connect different processing pipelines with only a small increase in complexity.

The delays are applied to the station data through complex multiplications and additions, programmed in assembly. In order to take full advantage of the L1 cache and the available registers, data is processed in sets of 6 stations, producing 3 beams, or a subset thereof to cover the remaining stations and beams. While the exact ideal set size in which the data is to be processed depends on the architecture at hand, we have shown in previous work that similar tradeoffs exist for similar problems across different architectures [3, ?].

Because each beam is an accumulation of the data from all stations, the bandwidth of each beam is equal to the bandwidth of data from a single station, which is 6.2 Gb/s

now that the samples are 32-bit floats. Once the beams are formed, they are kept as XY polarisations or transformed into the Stokes IQUV or the Stokes I parameters. In the latter case, the beams can also be integrated time-wise, in which groups of samples of fixed size are accumulated to reduce the resulting data rate.

The beamformer transforms chunks representing station data into chunks representing beam data. Because a chunk representing station data contained data for only one subband, the chunks representing different subbands of the same beam are still spread out over the full BG/P. Chunks corresponding to the same beam are brought together using a second all-to-all exchange.

6.5 Channel-level Dedispersion

Another major component in the pulsar-observation pipeline is real-time dedispersion. Since light of a high frequency travels faster through the interstellar medium than light of a lower frequency, the arrival time of a pulse differs for different wave lengths. To combine data from multiple frequency channels, the channels must be aligned (shifted in time). Otherwise, the pulse will be smeared or even overlap with the next pulse, causing many details to be lost. This process, called *dedispersion*, is done by post-processing software that runs after the observation has finished. However, to observe at the lowest frequencies, or to observe fast-rotating millisecond pulsars, dedispersion must also be performed *within* a channel, since our channels (typically 12 kHz) are too wide to ignore dispersion.

Figure 4 illustrates pulses of pulsar J0034-0534 at four frequencies. The pulse period is 1.88 ms. On the left is the original dispersed signal, which results in a smeared pulse when the frequencies are collapsed into a 12 kHz channel. On the right is the dedispersed signal, which results in a sharp pulse when collapsed.

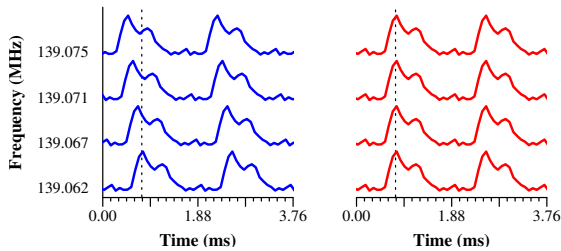


Fig. 4. Pulse arrival times within a 12 kHz channel before (left) and after (right) channel-level dedispersion.

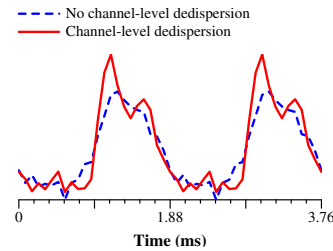


Fig. 5. Pulse profiles with and without channel-level dedispersion.

Dedispersion is performed in the frequency domain, effectively by doing a 4096-point Fourier transform (FFT) that splits a 12 kHz channel into 3 Hz subchannels. The phases of the observed samples are corrected by applying a chirp function, i.e., by multiplication with precomputed, channel-dependent, complex weights. These multi-

plications are programmed in assembly, to reduce the computational costs. A backward FFT is done to revert to 12 kHz channels.

Figure 5 shows the observed effectiveness of channel-level dedispersion, which improves the effective time resolution from 0.51 ms to 0.082 ms, revealing a more detailed pulse and a better signal-to-noise ratio. Dedispersion thus contributes significantly to the data quality, but it also comes at a significant computational cost due to the two FFTs it requires. It demonstrates the power of using a *software* telescope: the pipeline component was implemented, verified, and optimized in only one month time.

6.6 Second All-to-all Exchange

In the second all-to-all exchange, the chunks made by the beamformer are again exchanged over the 3D-torus network. Due to memory constraints on the compute cores, the cores that performed the beam forming cannot be the same cores that receive the beam data after the exchange. We assign a set of cores (*output cores*) to receive the chunks. The output cores are chosen before an observation, and are distinct from the *input cores* which perform the earlier computations in the pipeline.

An output core gathers the chunks that contain different subbands but belong to the same slice (see Section 5). Then, it rearranges the dimensions of the data into their final ordering, which is necessary, because the data order that will be written to disk is not the same order that can be produced by our computations without taking heavy L1 cache penalties. We hide this reordering cost at the output cores by overlapping computation (the reordering of a chunk) with communication (the arrival of other chunks). Once all of the chunks are received and reordered, they are sent back to the I/O node.

For the distribution of the workload over the available output cores, three factors have to be considered. First, all of the data belonging to the same beam has to be processed by output cores in the same pset, to ensure that one I/O node can concatenate all of the 0.25 second chunks that belong to the beam. Second, the maximum output rate per I/O node has to be respected. Finally, the presence of the first all-to-all exchange, which uses the same network at up to 198 Gb/s. The second exchange uses up to 80 Gb/s. Even though each link sustains 3.4 Gb/s, it has to process the traffic from four cores, as well as traffic routed through it between other nodes. The network links in the BG/P become overloaded unless enough output cores are used to spread the load.

6.7 Transport to Disks

Once an output core has received and reordered all of its data, the data are sent to the core's I/O node. The I/O node forwards the data over TCP/IP to the storage cluster. To avoid any stalling in our pipeline due to network congestion or disk issues, the I/O node uses a best-effort buffer which drops data if it cannot be sent.

7 Performance Analysis

We will focus our performance analysis on edge cases that are of astronomical interest. In all cases, we respect the real-time nature of our system by limiting the load such that

there is at most 0.1% of data loss. Almost all variance occurs in the networks within the BG/P due to clashes caused by scheduling intricacies.

7.1 Overall Performance

Figure 7.2 shows the maximum number of beams that can be created when using a various number of stations, in each of the three modes: Complex Voltages, Stokes IQUV, and Stokes I. In both the Complex Voltages and the Stokes IQUV modes, the pipeline is I/O bound. Each beam is 6.2 Gb/s wide. We can make at most 12 beams without exceeding the available 80 Gb/s to our storage cluster. The available bandwidth decreases down to 70 Gb/s due to the fact that an I/O node can only output 1.1 Gb/s if it also has to process station data. The granularity with which the output can be distributed over the I/O nodes, as well as scheduling details, determine the actual number of beams that can be created, but in all cases, the beamformer can create at least 10 beams at LOFAR’s full observational bandwidth.

In the Stokes I mode, we applied several integration factors (1, 2, 4, 8, and 12) in order to show the trade-off between beam quality and the number of beams. Integration factors higher than 12 does not allow significantly more beams to be created, but could be used in order to further reduce the total output rate. For low integration factors, the beam former is again limited by the available output bandwidth. Once the Stokes I streams are integrated sufficiently, the system becomes bounded by the compute nodes: if only signals from a few stations have to be combined, the beam former is limited by the amount of available memory required to store the beams. If more input has to be combined, the beam former becomes limited by the CPU power available in the compute cores. For observations for which a high integration factor is acceptable, the beam former is able to create 155 up to 543 tied-array beams, depending on the number of stations used. For observations which need a high time resolution and thus a low integration factor, the beam former is still able to create at least 42 tied-array beams.

7.2 System Load

We further analyse the workload of the compute cores by highlighting a set of cases, summarised in Table 1. We will focus on a memory-bound case (A), which also creates the highest number of beams, on CPU-bound cases interesting for performing surveys, with either 24 stations (B) or 64 stations (C) as input. Cases D and E focus on high-resolution observations of known sources, and are I/O bound configurations with 24 and 64 stations, respectively. Case F focusses on the observations of known sources as well, using Stokes I output, which allows more beams to be created. Channel-level dedispersion is applied for all cases that observe known sources.

The workload of the compute cores for each case is shown in Figure 7.2, which shows the average workload per core. For the CPU-bound cases B and C, the average load has to be lower than 100% in order to prevent fluctuations from slowing down our real-time system. These fluctuations typically occur due to clashes within the BG/P 3D-torus network which is used for both all-to-all-exchanges, and cannot be avoided in all cases.

| Case | Mode | Channel dedisp. | Int. factor | Stations | Beams | Input rate | Output rate | Bound | Used for |
|------|-------------|-----------------|-------------|----------|-------|------------|-------------|--------|---------------|
| A | Stokes I | N | 12 | 4 | 543 | 12 Gb/s | 70 Gb/s | Memory | Surveys |
| B | Stokes I | N | 8 | 24 | 327 | 74 Gb/s | 63 Gb/s | CPU | Surveys |
| C | Stokes I | N | 8 | 64 | 155 | 198 Gb/s | 30 Gb/s | CPU | Surveys |
| D | Stokes IQUV | Y | - | 24 | 13 | 74 Gb/s | 80 Gb/s | I/O | Known sources |
| E | Stokes IQUV | Y | - | 64 | 10 | 198 Gb/s | 62 Gb/s | I/O | Known sources |
| F | Stokes I | Y | 1 | 64 | 42 | 198 Gb/s | 65 Gb/s | CPU | Known sources |

Table 1. Several highlighted cases.

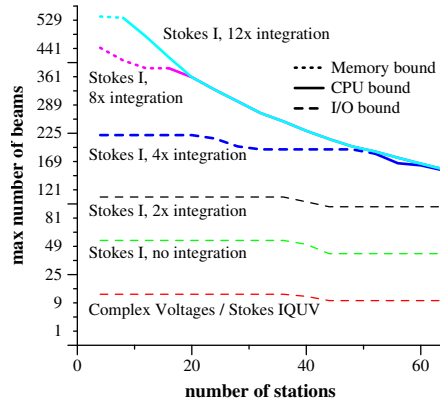


Fig. 6. The maximum number of beams that can be created in various configurations.

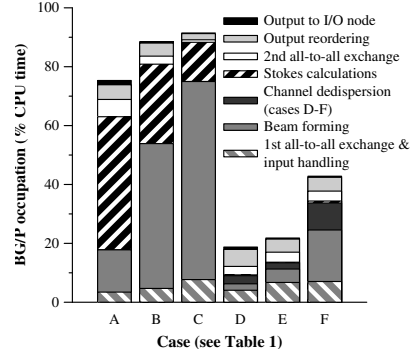


Fig. 7. The time spent in the processing steps.

The cases which create many beams (A-C) spend most of the cycles performing beam forming and calculation the Stokes I parameters. The beamforming scales with both the number of stations and the number of beams, while the Stokes I calculation costs depends solely on the number of beams. Case A has to beam form only four stations, and thus requires most of its time calculating the Stokes I parameters. Case B and C use more stations, and thus need more time to beam form.

The costs for both the first and the second all-to-all exchange are mostly hidden due to overlaps with computation. The remaining cost for the second exchange is proportional to the output bandwidth required in each case.

For the I/O-bound cases D-F, only a few tied-array beams are formed and transformed into Stokes I(QUV) parameters, which produces a lot of data but requires little CPU time. Enough CPU time is therefore available to include channel-level dedispersion, which scales with the number of beams and, as Figure 7.2 shows, is an expensive operation.

8 Discussion

9 Conclusions

References

1. A.G. de Bruyn et al. Exploring the Universe with the Low Frequency Array, A Scientific Case, September 2002.
<http://www.lofar.org/PDF/NL-CASE-1.0.pdf>.
2. J.W.T. Hessels, S.M. Ransom, I.H. Stairs, P.C.C. Freire, V.M. Kaspi, and F. Camilo. A Radio Pulsar Spinning at 716 Hz. *Science*, 311(5769):1901–1904, March 2006.
3. R.V. van Nieuwpoort and J.W. Romein. Using Many-Core Hardware to Correlate Radio Astronomy Signals. In *ACM International Conference on Supercomputing (ICS'09)*, pages 440–449, New York, NY, June 2009.
4. J.W. Romein. FCNP: Fast I/O on the Blue Gene/P. In *Parallel and Distributed Processing Techniques and Applications (PDPTA'09)*, Las Vegas, NV, July 2009.
5. J.W. Romein, P.C. Broekema, J.D. Mol, and R.V. van Nieuwpoort. The LOFAR Correlator: Implementation and Performance Analysis. In *ACM SIGPLAN Symposium on Principles and Practice on Parallel Programming (PPoPP'10)*, Bangalore, India, January 2010. To appear.
6. IBM Blue Gene team. Overview of the IBM Blue Gene/P Project. *IBM Journal of Research and Development*, 52(1/2), January/March 2008.
7. K. Yoshii, K. Iskra, H. Naik, and P.C. Broekema P. Beckman. Performance and Scalability Evaluation of “Big Memory” on Blue Gene Linux. *International Journal of High Performance Computing*. To appear.